



Interference fringes in plane-wave topography of $\text{Al}_x\text{Ga}_{1-x}\text{As}$ epitaxial layers implanted with Se ions

W. Wierzchowski^{a,*}, K. Wieteska^b, W. Graeff^c, A. Turos^a

^a*Institute of Electronic Materials Technology, Wólczyńska 133, 01-919 Warsaw, Poland*

^b*Institute of Atomic Energy, 05-400 Otwock-Świerk, Poland*

^c*HASYLAB at DESY, Notkestraße 85, D-22603 Hamburg, Germany*

Abstract

The MOCVD grown $\text{Al}_{0.45}\text{Ga}_{0.55}\text{As}$ epitaxial layers with low dislocation density, implanted with 1.5 MeV Se^+ ions to the doses $6 \times 10^{13} - 4 \times 10^{14}$ ions/cm², were studied using a multicrystal arrangement and applying synchrotron X-ray radiation. A very small size of the probe beam close to 30 μm was used to obtain a good resolution of interference maxima and to study the changes of the rocking curves in different regions of the sample. Due to the curvature of the samples, the interference maxima were revealed in plane wave topographs as interference fringes and the high intensity of the source enabled studying of the fringes also in these regions of the curve where the reflected intensity is very low. The continuity of the fringes across the boundary of implanted region was observed for the high angle side of the maximum due to epitaxial layer. A good approximation of experimental rocking curves and fringe pattern in the plane-wave topographs was obtained by numerical integration of the Takagi–Taupin equations assuming a strain profile with almost constant lattice parameter in a relatively thick layer close to the surface. © 1999 Elsevier Science B.V. All rights reserved.

Keywords: Ion implantation; $\text{A}^{\text{III}}\text{B}^{\text{V}}$ semiconductors; X-ray interference phenomena

1. Introduction

The implantation induced effects are not yet well known in the case of different multicomponent semiconductor compounds. Most numerous papers [1–3] concern mainly $\text{Al}_x\text{Ga}_{1-x}\text{As}$ which is the most commonly commercially used material. The mentioned papers include the use of X-ray measurements and, in particular, the recording of the rocking curves. The curves presented in the case of the multicomponent semiconductors are strongly affected by pre-existing dislocation structure and by the curvature of the samples strongly decreasing visibility of the interference maxima in comparison with the results obtained for bulk silicon [4,5] and gallium arsenide [6,7]. Despite the possibility of successful including of the effects caused by dislocation structure [6,7], they always mask the information about the strain profile obtainable from the rocking curves.

In the present investigation, two important precautions were introduced for better recognition of implantation induced effects in $\text{Al}_x\text{Ga}_{1-x}\text{As}$ implanted with 1.5 MeV Se^+ ions to a wide range of doses. Firstly, the dislocation density was significantly reduced by using a highly indium

doped substrate material with low dislocation density. Secondly, the use of multicrystal arrangement and synchrotron X-ray source enabled reducing the probe beam to a very small size providing also an excellent collimation of the beam. The numerical simulation based on the Takagi–Taupin theory was used for analysis of the results. Some preliminary results obtained for the same samples were presented at SIMC-X conference in Berkeley [8].

2. Experimental

The $\text{Al}_{0.45}\text{Ga}_{0.55}\text{As}$ epitaxial layers were deposited with MOCVD method on (100) oriented substrates cut out from Bridgman grown GaAs crystal isoelectronically doped with 0.3% indium and contained less than 10^3 cm⁻² dislocations. The layers were 3 μm thick and 0.2 μm of undoped GaAs buffer layer was initially deposited. The substrates allowed growth of the layers with similar low dislocation density partly because of lower misfit factor due to their greater lattice parameter. The value of this parameter was determined as 6.5344 Å by means of modified Bond method proposed by Godwod et al. [9]. As it was revealed by means of X-ray topography only single misfit dislocations occurred locally in some areas of the

*Corresponding author.

samples. The implantation with 1.5 MeV Se^+ ions was performed at Rossendorf Research Centre at room temperature. The ion doses covered range from 6×10^{13} to 4×10^{14} ions/cm². The 6° inclination of the sample was applied to eliminate channelling effects.

The synchrotron experiments were performed using RÖMO-1 piezoelectrically stabilised double-crystal monochromator at HASYLAB. The 1.1-Å radiation was selected and 400 symmetrical reflection was set in the investigated crystals. The high intensity of the source in the selected spectral range allowed reducing the probe beam size to less than 30 μm significantly decreasing the influence of the curvature and sample inhomogeneities. The completion of synchrotron experiments were measurements of rocking curves in 511 $\text{CuK}\alpha$ reflection using conventional double-crystal spectrometer.

The synchrotron investigation included also the plane wave topography with wide monochromatized beam. Due to crystal curvature, we obtained distinct fringes corresponding to the interference maxima in the rocking curves. The high intensity of the beam enabled taking topographs corresponding to the region of the curve where the reflected intensity is very low.

3. Numerical simulation

The numerical simulations were performed by direct numerical integration of the Takagi–Taupin equations. In the case of rocking curves, the form of Takagi–Taupin equations assuming the solution dependent on the vertical coordinate only was integrated by the half-step derivative method similarly as in [5]. In the calculation, we took into account the chemical composition, epitaxial layer profile and presence of the buffer layer.

As it was mentioned in [7,8], the approximation of the strain by vacancy distribution profile obtained using TRIM-95 program, which was very successful in the case of high-energy implantation into silicon [4,5], was inadequate and produced less distinct implanted layer maximum. This fact evidently pointed that the implanted layer is thicker with a much lower variation of the lattice parameter. The appropriate profiles were obtained from the TRIM-95 vacancy profiles using two following operations, which to some extent may be explained by the expected vacancy diffusion.

In the first operation, the TRIM-95 vacancy profile was treated as initial distribution, which may be modified by the diffusion. The transformation of this profile was then realised solving numerically one-dimensional diffusion equation. This operation could increase the depth of the vacancy distribution but it still does not produce expected flattening of the top part. The second operation consisted on taking the sine function of the modified profile. It seems to be reasonable in view of observed character of lattice parameter changes known to reach maximum at the dose 2×10^{14}

ions/cm² [1,8]. This dependence of lattice parameter change on the dose may be approximated by a part of sine function. It may be than expected that similar behaviour of lattice parameter change may concern also its depth distribution.

The simulation experiments included taking into account damage-caused decrease of the structure factor corresponding to the stopping power distribution, proposed by some authors [6,7]. This correction caused small changes in intensity of main maxima but did not change the position of the interference maxima. Hence the use this correction does not seem to be absolutely necessary.

4. Results and discussion

As it was found in a number of topographic investigations, the examined layers were of very good crystallographic quality and contained a similar dislocation density as the substrates. The proof of the good quality of the layers is the presence of interference maxima shown representatively in Fig. 1. At the present thickness of the layer close to 3 μm these fringes are relatively narrow and cannot be observed in samples of poor structural quality.

The set of curves corresponding to three increasing doses is shown in Fig. 2a–c. The general feature of the rocking curves recorded in investigated implanted layers was the presence of an additional distinct maximum corresponding to the implanted layer. The second and third maximum correspond to the maxima of the curve shown in Fig. 1 measured for not implanted epitaxial layer but the second maximum is now less intense as it corresponds to a not penetrated part of epitaxial layer. The curves confirm a

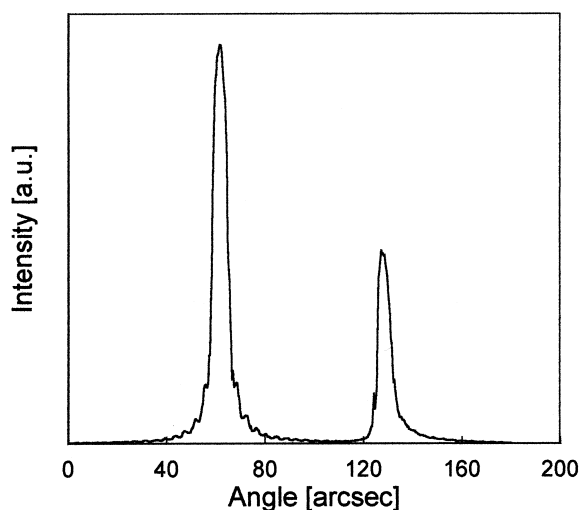


Fig. 1. The rocking curve recorded using multicrystal arrangement with synchrotron X-ray radiation in 400 reflection of 1.1 Å of not implanted $\text{Al}_{0.45}\text{Ga}_{0.55}\text{As}$ epitaxial layer, showing distinct interference maxima on both sides of the layer maximum and also on high angle side of the substrate maximum.

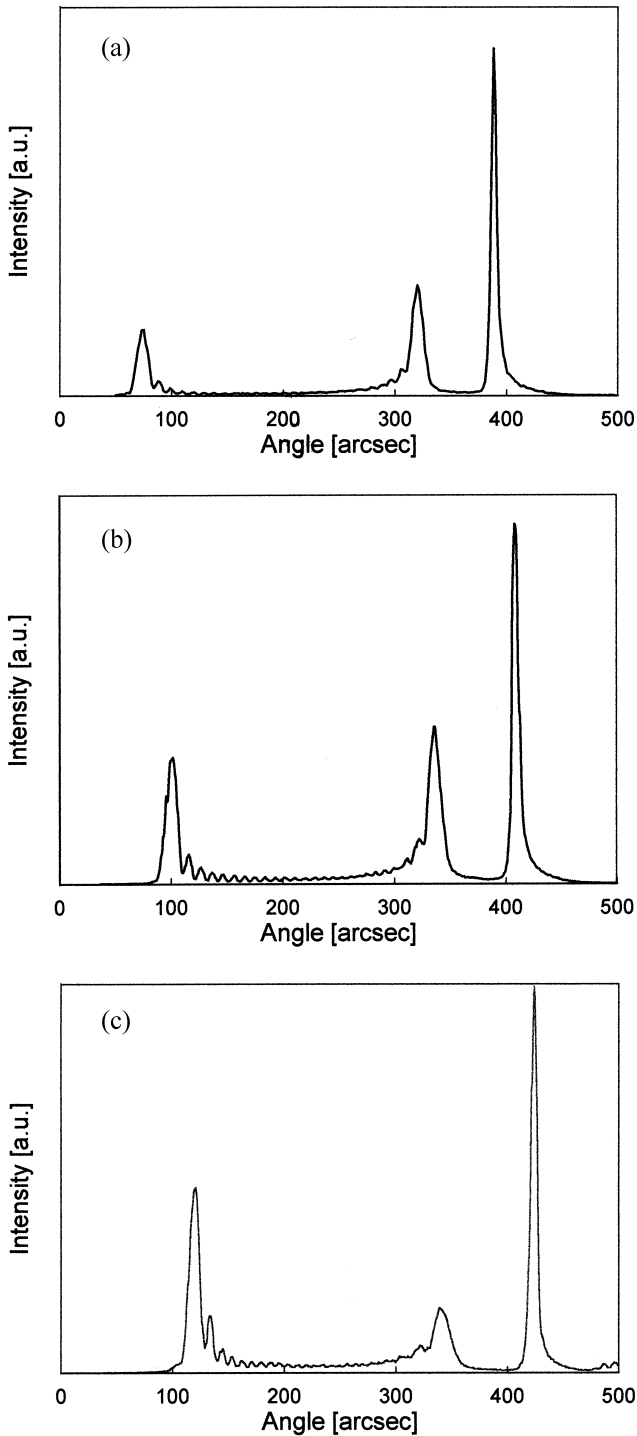


Fig. 2. The rocking curve recorded using multicrystal arrangement with synchrotron X-ray radiation in 400 reflection of 1.1 Å for $\text{Al}_{0.45}\text{Ga}_{0.55}\text{As}$ epitaxial layers implanted with various doses of 1.5 MeV Se ions: (a) to the dose 1.8×10^{14} ions/cm², (b) to the dose 2.4×10^{14} ions/cm², and (c) to the dose 4×10^{14} ions/cm².

significant change of lattice spacing and tetragonal deformation caused by Se^+ implantation. The difference in lattice parameter between the epitaxial layer and the substrate was 3–4 times smaller. It is noteworthy that the

distance between the first and second maximum, which is the measure of implantation induced lattice parameter change, reaches its maximum between second and third curve at the dose close to 2×10^{14} ions/cm². The angular distance between the second and third maximum is the same in all curves.

The relation of height of the first maximum to the height of the other maxima does not exhibit any distinct regularity. More characteristic is the systematic decrease of the maximum coming from the unaffected part of the epitaxial layer. That points the increase of the disturbed layer thickness with ion dose.

The rocking curves exhibit distinct interference maxima especially well pronounced in the region between the first and the second main maximum. The maxima are, however, present even in the tail behind the third maximum being not well resolved in the curves but, as it will be shown further, they are very well visible in the plane-wave topographs as the interference fringes.

The representative synchrotron plane-wave topographs are shown in Fig. 3. As it was already mentioned, due to the curvature of the presently investigated samples exhibiting curvature radius in the range 25–40 m, the different regions in the particular topograph correspond to different regions of the rocking curve. In Fig. 3 the vertical direction along the diffraction plane corresponds to lowering Bragg angle. The topographs in Fig. 3 were taken respectively in the vicinity of the first, second and third maximum of the sample implanted with the doses 1.8×10^{14} ions/cm². The topographs allow following the correspondence of the fringes on the two sides of implanted region boundary.

The topographs allow resolving of even more details than in the case of rocking curves recorded with the probe beam side limited to 30 μm. The worth noting feature is almost complete correspondence in the fringe position on both sides of implanted area boundary for the high angle side of the second main maximum. According to well known theory of diffraction in thin layers [10] this fact may be explained as follows. Far from the maximum due to implanted layer the dominant diffraction phenomenon is the reflection of the wave-field from the boundary between the epitaxial layer and substrate. This phenomenon is enhanced by the presence of the buffer layer with the reflection maximum moved toward higher angles.

As it is illustrated in Figs. 4 and 5, the procedure described in former paragraph was quite successful in obtaining simulated curves reproducing many features of experimental ones shown in Fig. 2. The used strain profiles are shown in Fig. 5 together with initial vacancy depth distribution profile and the intermediate profiles obtained after different assumed diffusion types. The final profiles were obtained using in argument of the sine function the factor increasing with the dose. As it was already mentioned many features of the profiles shown in Fig. 5 were confirmed by the RBS/channelling measurements, which

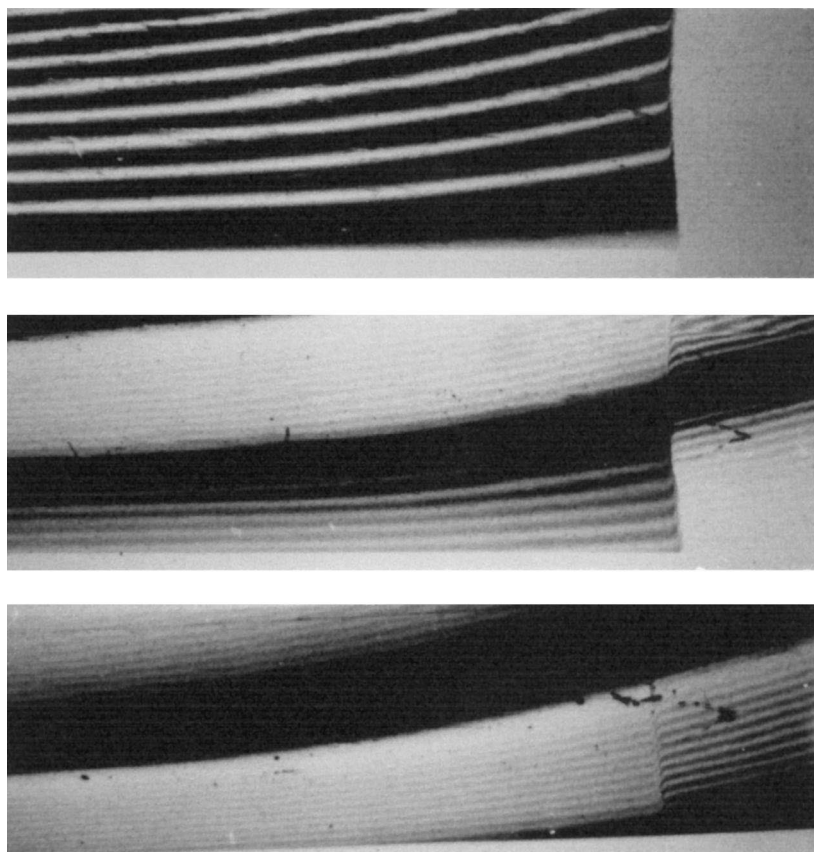


Fig. 3. The synchrotron plane wave topographs in 400 reflection of 1.1 \AA radiation for the $\text{Al}_{0.45}\text{Ga}_{0.55}\text{As}$ epitaxial layers sample implanted with 1.5 MeV Se ions to the dose 1.8×10^{14} ions/cm²: (a) for angular setting in the vicinity of implanted layer maximum, (b) for angular setting in the vicinity of epitaxial layer maximum, (c) for angular setting in the vicinity of substrate maximum. The left part of the topographs reveals the implanted area and the upper direction corresponds to the increasing glancing angle.

will be published separately. It should be stressed that systematic increase of the penetrated layer depth cannot be explained by channelling effects, as the higher concentration of introduced points defects will disturb the eventual channelling phenomena.

5. Conclusions

The use of highly perfect indium doped substrates and multicrystal arrangement with synchrotron X-ray source enabled effective observation of diffraction profiles introduced by 1.5 MeV Se implantation to epitaxial $\text{Al}_{0.45}\text{Ga}_{0.55}\text{As}$ layers. The obtained curves exhibit distinct interference maxima, which were also revealed as fringes in plane wave topographs.

The recorded rocking curves show that the depth range of lattice parameter changes is more than 1.5 times larger than that coming from the TRIM-95 Monte Carlo calculation and the near surface region of the implanted layers seems

to have almost constant lattice parameter. The strain profiles providing good correspondence with the experiment were obtained assuming the diffusion of the point defects, and the saturation of the lattice parameter changes proportional to the concentration to the dose of introduced defects.

The observed continuity of fringes through the implanted region boundary and its periodicity proves that the interference fringes on high angle side of the maximum due to epitaxial layer are connected with the reflection of the wave-fields from the buffer layer (top parts of the substrate).

Acknowledgements

The present work was supported by the State Committee for Scientific Research (grant 8 T11B 049 13) and Polish–German Agreement on Scientific Cooperation POL–GER–N-100-95/BO.

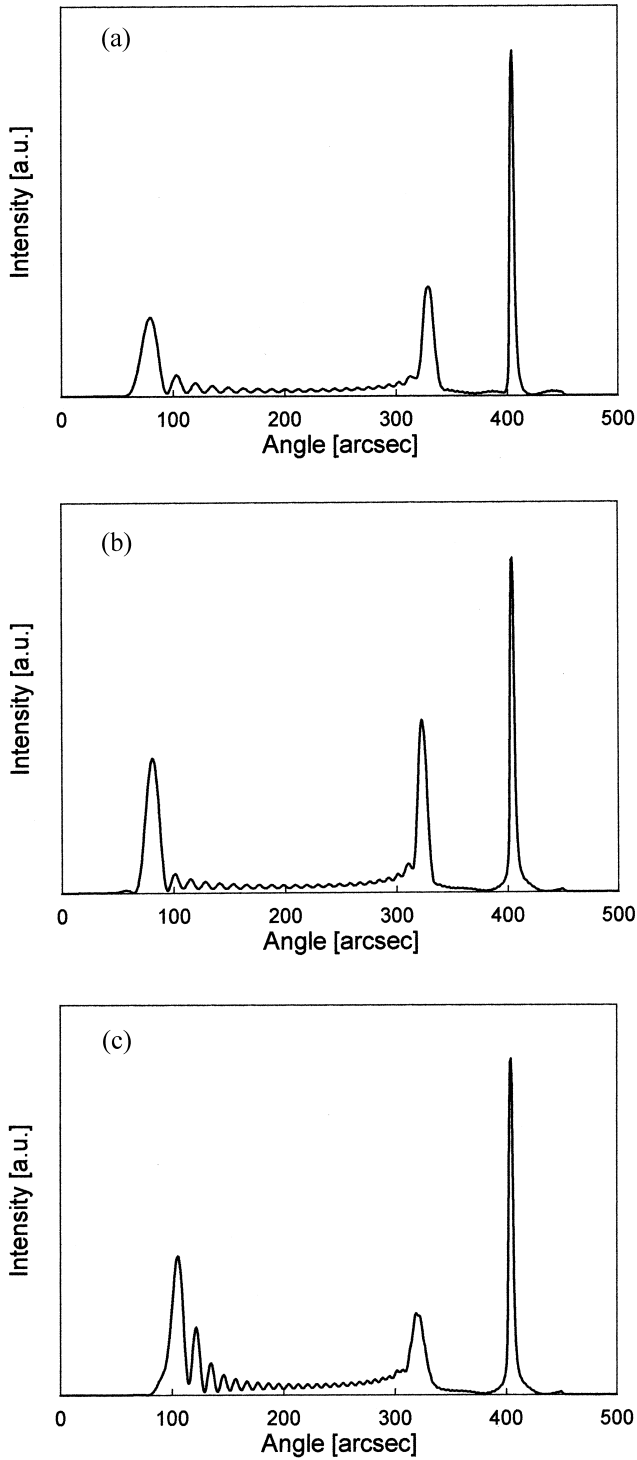


Fig. 4. (a–c) The simulated rocking curve corresponding to assumed model of obtaining lattice parameter depth distribution profiles.

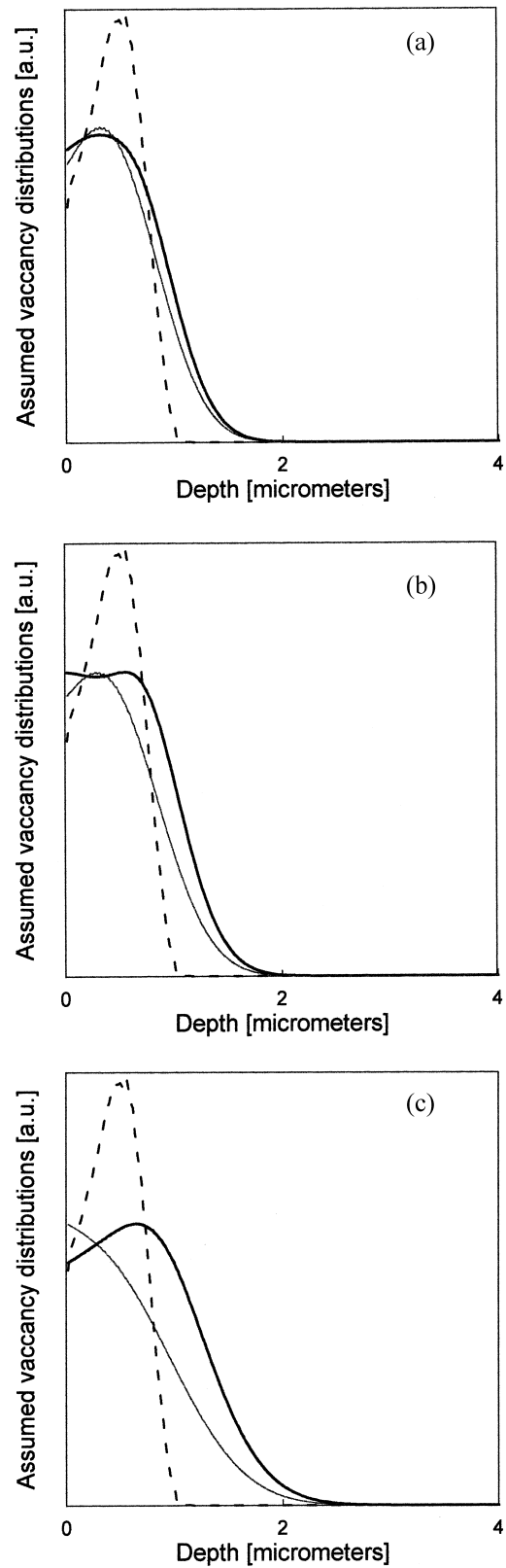


Fig. 5. Lattice parameter depth distribution profiles assumed in calculation of curves shown in Fig. 4, with the profiles corresponding to the different times of diffusion and initial vacancy distribution profiles obtained from TRIM-95 program drawn with thick, thin and dashed lines, respectively.

References

- [1] P. Partyka, R.S. Averback, J.J. Coleman, P. Erhart, W. Jäger, Mater. Res. Soc. Symp. Proc. 354 (1995) 219.
- [2] H.H. Tan, C. Jagadish, J.S. Williams, J. Zou, D.H.J. Cockayne, A. Sikorski, J. Appl. Phys. 77 (1995) 87.
- [3] B.A. Turkot, B.W. Lagow, I.M. Robertson, D.V. Forbes, J.J. Coleman, L.E. Rehn, P.M. Baldo, J. Appl. Phys. 80 (1996) 4366.
- [4] K. Wieteska, W. Wierzchowski, Phys. Stat. Sol. (a) 147 (1995) 55.
- [5] K. Wieteska, W. Wierzchowski, W. Graeff, K. Dłużewska, Phys. Stat. Sol. (a) 168 (1998) 11.
- [6] C.R. Wie, T.A. Tombrello, T. Vreeland, J. Appl. Phys. 59 (1986) 3743.
- [7] F. Xiong, C.J. Tsai, T. Vreeland, A. Tombrello, C.L. Schwartz, S. Schwartz, J. Appl. Phys. 69 (1991) 2964.
- [8] A. W. Wierzchowski, K. Wieteska, W. Turos, R. Greeff, in: SIMC-X 1988, 10th Conf. on Semiconducting and Insulating Materials, June 1–5, California Abstract Book, San Francisco, 1988, p. 2/16.
- [9] K. Godwod, Z. Szmid, J. Kowalczyk, Phys. Stat. Sol. (a) 21 (1974) 227.
- [10] B.M. Battermann, G. Hildebrandt, Acta Crystallogr. A24 (1968) 150.